Hydrochemical Tracing for Solute Sources and Enrichment Mechanisms in Inland Lake Waters of the Qiangtang Plateau, Northern Tibet, China

Yuanqing Liu , Dongguang Wen , Le Zhou , Lin Lv , Xuejun Ma , Jianhua Feng , Yanwei Guo , Jian Cao * , Tao Lv *

Posted Date: 19 May 2026

doi: 10.20944/preprints202605.1189.v1

Keywords: Tibetan plateau; hydrochemistry; hydrogeology; salt lake; ionic ratio

 doi:10.20944/preprints202605.1189.v1

Article

Hydrochemical Tracing for Solute Sources and Enrichment Mechanisms in Inland Lake Waters of the Qiangtang Plateau, Northern Tibet, China

Yuanqing Liu [1,2,†], Dongguang Wen [2], Le Zhou [2,†], Lin Lv [2], Xuejun Ma [2], Jianhua Feng [2], Yanwei Guo [2], Jian Cao [3,*] and Tao Lv [4,*]

[1] School of Water Resources and Environment, China University of Geosciences (Beijing), Beijing 100083, China

[2] Center for Hydrogeology and Environmental Geology, CGS, Tianjin 300309, China

[3] Tianjin Geological Research and Marine Geological Center, Tianjin 300170, China

[4] Shandong Provincial Geo-mineral Engineering Exploration Institute, Jinan 250014, China

* Correspondence: cjdyhy@126.com (J.C.); lvtao@sd-gold.com (T.L.)

† These authors contributed equally to this work.

Abstract

To reveal the solute sources, migration and enrichment mechanisms of water bodies in the endorheic lake region of the Qiangtang Plateau, Tibetan Plateau, and to clarify the hydrogeochemical cycling patterns in alpine arid zones, this study took typical endorheic lake areas in the region as the research object, conducted a systematic hydrogeological survey, collected 28 groups of water samples of various types (including springs, rivers, thermal springs, freshwater lakes, salt lake brines, atmospheric precipitation and glacial meltwater), tested their major ions, trace elements and physical properties, and comprehensively investigated the hydrogeochemical characteristics, evolution laws and solute sources of water bodies, quantified the dominant controlling factors and established a conceptual hydrogeochemical model by combining methods such as PHREEQC modeling, principal component analysis (PCA) and Pearson correlation analysis; the results show that water bodies in the study area exhibit a distinct evolutionary gradient, from the low-salinity HCO_3-Ca recharge end-member, through transitional $HCO_3 \cdot SO_4$-Ca(Mg) water, to highly mineralized Cl-Na(SO_4·Cl-Na) salt lake brine, with synchronous enrichment of Li, B, As and other elements; solute sources are controlled by a ternary coupling mechanism of evaporative concentration, rock weathering and leaching, and deep geothermal fluid input, while cation exchange and mineral dissolution-precipitation further regulate ionic ratios; As, Li, B and Cl^- display conservative migration in non-hydrothermal waters, whereas thermal springs show unique geochemical signatures due to the input of deep-seated fluids; PCA reveals that evaporative concentration (contribution rate 55.39%) is the dominant controlling factor, rock weathering (17.09%) provides the basic solute load, and the coupled process of deep fluid mixing and carbonate precipitation (14.21%) regulates elemental fractionation, and this study constructs a conceptual model of "multi-source recharge–water–rock interaction–evaporative concentration", which clarifies the evolutionary laws of regional water bodies and provides a scientific basis for water cycle research and green exploration of strategic mineral resources in salt lakes of the endorheic regions on the plateau.

Keywords: Tibetan plateau; hydrochemistry; hydrogeology; salt lake; ionic ratio

1. Introduction

Known as the "Asian Water Tower", the Tibetan Plateau is the source of numerous major rivers, including the Yangtze, Yellow, and Lancang Rivers. Its unique alpine climate, active geological structures, and extensive permafrost have collectively shaped a complex and fragile

 doi:10.20944/preprints202605.1189.v1

hydrogeochemical environment [1–3]. As the highest and largest plateau on Earth, its groundwater system plays an irreplaceable role in maintaining the flow stability of major Asian rivers, safeguarding the health of regional ecosystems, and ensuring the water security of hundreds of millions of people [4]. Located in the core hinterland of the Tibetan Plateau, the Qiangtang Plateau hosts the world's highest-altitude and most densely distributed endorheic lake groups, dominated by salt lakes and saline lakes. These lakes not only serve as the terminal of the regional hydrological cycle but also form a large natural "resource reservoir" enriched with strategic critical metal elements such as Li, B, K, Rb, and Cs [5–7]. Against the backdrop of global carbon neutrality and energy transition, systematically elucidating the solute sources, migration processes, and enrichment mechanisms of water bodies in the Qiangtang endorheic lake region is crucial for advancing our understanding of hydrogeochemical cycles in alpine arid zones, evaluating climate change impacts, and guiding mineral resource exploration.

Current studies on solute sources and evolution mechanisms of water bodies on the Tibetan Plateau have focused separately on exorheic river basins and endorheic lake regions [8]. For exorheic basins represented by the Yarlung Zangbo and Lancang Rivers, previous research has revealed the contributions of silicate weathering, carbonate weathering, and evaporite dissolution to river hydrochemistry, as well as their regulatory roles in the global carbon cycle [9–11]. In contrast, studies on endorheic basins (e.g., the Qaidam Basin and southern Tibet salt lake regions) have concentrated on the genesis and evolution of Li-rich and B-rich brines, highlighting the key controlling effects of geothermal activity, volcanic rock weathering, and deep fluid input on salt lake ore-forming materials [12–14]. Hydrochemical composition and ionic ratio analysis, a classic and effective approach, can effectively identify the contributions of different sources and reveal key processes such as water-rock interaction through the compositional characteristics of major ions (e.g., Ca^{2+}, Mg^{2+}, Na^{+}, K^{+}, HCO_3^{-}, SO_4^{2-}, Cl^{-}) [15–18]. However, most existing studies focus on individual river or salt lake systems, leaving a gap in our systematic understanding of the regional distribution of water solutes, quantitative identification of multiple sources, and enrichment mechanisms under varying hydrogeological conditions in the vast Qiangtang endorheic lake region.

The Qiangtang endorheic lake region, characterized by a typical alpine arid climate, closed topographic setting, active tectonic activity, and extensive thermal spring outcrops, serves as a natural laboratory for investigating solute sources and enrichment [19,20]. Widely distributed Quaternary lacustrine sediments, ophiolite suites, and granite intrusions in this region provide a complex background for water-rock interaction [21,22]. Meanwhile, significant differences in salinity, hydrochemical types, and key element abundances among different lakes suggest that their solute sources and evolution pathways may be governed by distinct mechanisms. For instance, although Lakko Co and Mami Co are spatially adjacent, their Li sources differ substantially: the former is primarily recharged by Li-rich geothermal springs, while the latter relies more on the weathering and leaching of Li-rich silicate rocks within its basin [23–25]. These differences indicate that single-lake or single-river studies are insufficient to fully capture the complex behaviors of water solutes in the Qiangtang endorheic lake region, highlighting the urgent need for comprehensive, cross-basin hydrochemical tracing studies integrating multiple elements.

Accordingly, this study selects multiple lakes and water systems in typical endorheic lake areas of the Qiangtang Plateau as research objects. Surface water, groundwater, and geothermal water samples were systematically collected, and hydrochemical composition and ionic ratio analysis were employed to achieve three objectives: (1) clarify the solute composition characteristics and spatial distribution patterns of different water bodies; (2) quantitatively identify the contributions of different sources to solutes; and (3) reveal the migration processes and enrichment mechanisms of key elements from source areas to lakes. The findings of this study will provide new insights into hydrological cycle processes and salt lake metallogenic theory in the Tibetan Plateau endorheic region, and offer scientific support for the green exploration and sustainable utilization of critical mineral resources.

 doi:10.20944/preprints202605.1189.v1

2. Geological Background

The Qinghai-Tibet Plateau is currently the highest, largest and youngest continent-continent collisional orogenic belt on Earth [26,27]. During successive continent-continent collision events, the Yarlung Zangbo Suture (YS), Bangong-Nujiang Suture (BS) and Jinsha River Suture (JS) developed sequentially from south to north across the Qinghai-Tibet Plateau. These three sutures together divide the Tibetan region into four major continental blocks, namely the Gangdese-Nyainqentanglha Block (GNB), Qiangtang-Sanjiang Composite Block (QSCB), and Himalayan Block (HMB) (Figure 1) [28,29].

The endorheic lake region of the Qiangtang Plateau is tectonically located across the Bangong-Nujiang Suture (BS, between Fault ① and Fault ②), the Gangdese-Nyainqentanglha Block (south of Fault ②) and the Qiangtang-Sanjiang Composite Block (north of Fault ①). The stratigraphic strikes in the region are consistent with the main structural lines, and are generally distributed in a NWW-trending direction. According to specific tectonic divisions and stratigraphic characteristics, different lake groups in the study area can be further subdivided: Lakes such as Dong Co and Xiaga Co are located within the Bangong-Nujiang Suture Zone (BNSZ), which is composed of slates, silt-fine sandstones and a small amount of ophiolite fragments from the Mugangri Group (JM); Lakes such as Berieze Co and Darao Co belong to the Bairuo Co-Wuma magmatic island arc belt (between Fault ② and Fault ③), which is characterized by island arc magmatism and active continental margin deposition, and the sedimentary successions mainly include silt-fine sandstones and shales of the Duoren Formation (J_3d) and Risong Formation (J_3r), as well as pyroclastic rocks of the Qushenla Formation (K_1q); Lakes such as Lakko Co, Mami Co and Guopu Co are located in the Ciding Co-Mami Co composite back-arc basin, whose sedimentary successions are dominated by clastic rocks of the Duoni Formation (K_1d) and carbonate rocks of the Langshan Formation (K_1l) and Xiala Formation (P_1x) (Figure 1).

 doi:10.20944/preprints202605.1189.v1

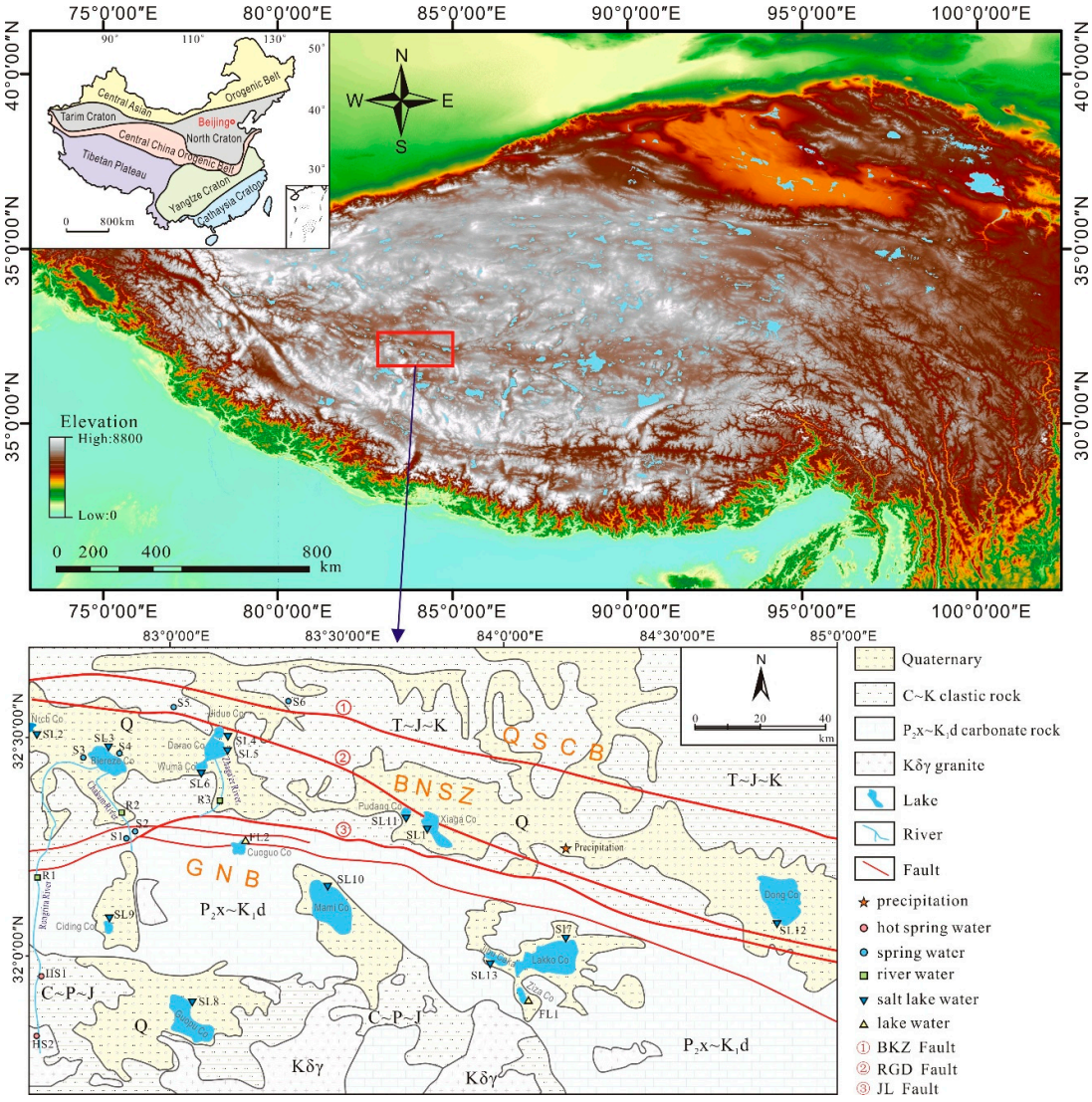

Figure 1. Schematic diagram of the location, geological overview, and sampling points of the research area.

The study area is located in Gaize County and Geji County in the hinterland of the Qiangtang Plateau, Xizang, with geographic coordinates of 31°40′00″-32°40′00″N and 82°40′00″-85°00′00″E (Figure 1). The study area is composed of seven closed independent lake-basin watershed units consisting of 13 saline and saltwater lakes (e.g., Dong Co, Laguo Co, Wuma Co, Berieze Co) and two freshwater lakes (Cuoguo Co, Xizha Co). The study area has a plateau subfrigid arid monsoon climate, characterized by severe cold, aridity, thin air, low pressure and oxygen deficiency, with a large diurnal temperature difference (usually ranging from 11 to 21 °C) and a long annual sunshine duration up to 3200 hours [30]. The annual precipitation is about 189.6 mm, the annual evaporation reaches 1870 mm, and the rainy season is concentrated from June to September [31]. The Xiagangjiang and Longge'er snow mountains (glaciers) are the highest elevations in the area, with main peak elevations of 6822 m and 6804 m respectively. Their abundant ice and snow meltwater forms the sources of major surface rivers such as Rongri'azangbo and Suomeizangbo (Figure 2f). During the runoff process, river water continuously recharges the lakes in the area through surface confluence and infiltration, becoming the most important water source and solute source for the lakes (Figure 2b, c). Controlled by tectonic conditions, part of the deep-source solutes continuously converge into surface rivers through karst springs and hot springs, and participate in the solute recharge and hydrochemical evolution of the lake water (Figure 2a,d,e).

 doi:10.20944/preprints202605.1189.v1

Figure 2. Field photographs of the study area. (a)Wenbudangsang karst spring(S1). (b)Biereze Co(SL3). (c)Rongria River(R1). (d) Hot springs near the JL Fault(HS1). (e) Hot springs upstream of the Rongria River(HS2). (f) Glaciers of the study area.

3. Sampling and Analytical Methods

In 2023, the China Geological Survey carried out hydrogeological surveys in the lake basin watershed of the southern Qiangtang Plateau, and a total of 28 water samples of various types were collected. All samples include: 6 freshwater spring samples, 3 river water samples, 2 hot spring samples (upstream of Berieze Co), 2 freshwater lake samples, 13 saline lake brine samples, 1 atmospheric precipitation sample and 1 glacial meltwater sample. The physical property indexes of the samples are listed in Table 1, and the sampling sites are shown in Figure 1. Sampling was conducted synchronously with on-site rapid water quality testing, and water samples were collected after the on-site parameters were stabilized. Water samples were filtered through 0.45 μm membranes and stored in polyethylene bottles; water samples for cation analysis were acidified in situ with nitric acid to pH < 2 to ensure component stability. All samples were analyzed in the laboratory of the Hydrogeology and Environmental Geology Center, China Geological Survey. In-situ measurements of water temperature, total dissolved solids (TDS), pH, dissolved oxygen (DO), electrical conductivity and oxidation-reduction potential (Eh) were performed using an in-Situ SMARTROLL multi-parameter water quality analyzer. Under laboratory conditions, major cations including Ca^{2+}, Mg^{2+}, Na^{+} and K^{+} were determined by flame atomic absorption spectrometry (FAAS); trace elements such as lithium (Li) and boron (B) were analyzed by inductively coupled plasma mass spectrometry (ICP-MS); HCO_3^- concentration was measured by acid-base indicator titration; and Cl^-, NO_3^- and SO_4^{2-} concentrations were determined using an ion chromatograph (IC883). Quality control was implemented through parallel sample analyses. The ion charge balance error (ICBE) was calculated according to Equation (1). The ICBE values of all water samples were controlled within ±5%, indicating that the analytical results are of high reliability.

$$\mathrm{ICBE}(\%) = \frac{\sum(Mg^{2+}+Ca^{2+}+Na^{+}+K^{+}) - \sum(HCO_3^-+SO_4^{2-}+NO_3^-+Cl^-+F^-)}{\sum(Mg^{2+}+Ca^{2+}+Na^{+}+K^{+}) + \sum(HCO_3^-+SO_4^{2-}+NO_3^-+Cl^-+F^-)} \quad (1)$$

Table 1. Sample type, description, and physical properties of samples (field collection).

No.	pH	T(℃)	Sample type	Description	Location
S1	8.99	12.75	Spring water	Wenbudangsang karst spring 1	N32°15′02.77″E 82°59′47.59″
S2	8.43	12.62	Spring water	Wenbudangsang karst spring 2	N32°15′20.28″E82°59′48.74″
S3	9.13	22.33	Spring water	Bieruoze Co west spring	N32°25′26.53″E82°52′27.07″
S4	8.41	10.77	Spring water	Bieruoze Co east spring	N32°25′58.41″E82°58′15.81″

 doi:10.20944/preprints202605.1189.v1

S5	8.45	12.35	Spring water	Source spring of Woqing River	N32°35′26.34″E83°06′54.97″
S6	7.75	17.67	Spring water	Source spring of Chongba River	N32°34′29.06″E83°23′17.45″
HS1	7.34	34.24	Hot spring water	Hot springs near the JL Fault	N 32°08′05.09″E 82°43′12.22″
HS2	7.46	48.55	Hot spring water	Hot springs upstream of the Rongria River	N 32°08′50.32″E 82°44′30.12″
R1	8.82	15.83	River water	Rongria River water	N32°18′23.01″E82°47′12.21″
R2	7.89	15.09	River water	Chakamu River water	N 32°20′33.74″82°55′54.67″
R3	7.99	14.44	River water	Zhaga'er River water	N32°20′08.49″E83°12′58.82″
FL1	9.88	18.22	Fresh lake water	Ziza Co Lake water	N31°55′55.81″E84°03′2.63″
FL2	8.52	15.04	Fresh lake water	Cuoguo Co Lake water	N32°16′06.24″E83°18′58.48″
SL1	9.28	20.21	Lake brine	Xiaga Co Lake brine	N32°16′26.72″E83°51′08.88″
SL2	8.84	19,56	Lake brine	Nrcb Co Lake brine	N32°31′09.64″E82°39′30.74″
SL3	9.29	18.69	Lake brine	Bieruoze Co Lake brine	N32°26′20.71″E82°57′42.81″
SL4	9.56	16.54	Lake brine	Jiduo Co Lake brine	N32°30′37.45″E83°12′32.58″
SL5	9.48	16.76	Lake brine	Darao Co Lake brine	N32°27′13.81″E83°11′21.01″
SL6	9.46	6.11	Lake brine	Wuma Co Lake brine	N32°26′07.21″E83°10′04.71″
SL7	9.46	15.85	Lake brine	Lakko Co Lake brine	N32°01′45.51″E84°03′31.83″
SL8	9.83	16.46	Lake brine	Guopu Co Lake brine	N31°53′52.09″E83°10′35.98″
SL9	8.80	17.45	Lake brine	Ciding Co Lake brine	N32°03′45.64″E82°56′39.69″
SL10	8.62	15.76	Lake brine	Mami Co Lake brine	N32°01′50.81″E83°32′58.81″
SL11	9.40	14.39	Lake brine	Pudang Co Lake brine	N32°20′17.04″E83°43′27.14″
SL12	9.34	11.75	Lake brine	Dong Co Lake brine	N32°09′29.02″E84°41′57.87″
SL13	9.19	16.59	Lake brine	Jibu Caka Lake brine	N32°00′46.04″E83°58′46.40″
Precipitation	8.12	/	/	Rain water	N32°17′57.58″E84°03′47.56″
Glacier	7.93	0.4	Glacier	Glacial meltwater	N32°15′34.39″E87°23′37.03″

4. Results

4.1. Hydrochemical Characteristics

As shown in Figure 3a,b, the ion concentrations and compositions of different water types in the study area exhibit significant differentiation, with obvious spatial variations also occurring within each water type. In terms of concentration levels, distinct differences exist among water bodies: general springs have the lowest overall ion concentrations; river water and freshwater lake samples display moderate ion concentrations with relatively uniform distributions; hot spring waters, influenced by geothermal processes, are significantly enriched in major ions (Na^+, K^+, Ca^{2+}, Mg^{2+}, Cl^-, HCO_3^-, SO_4^{2-}) and trace elements including Li, B, Sr and As; under intense evaporation and concentration, salt lake brines show exponentially elevated ion concentrations, with major ions and characteristic elements generally ranging from 10^2 to 10^5 mg/L, accompanied by strong spatial heterogeneity.

With respect to ionic composition, major ion components display systematic shifts with water type evolution: low-salinity waters such as precipitation, glacial meltwater, general springs and rivers are dominated by HCO_3^- as the major anion and Ca^{2+} and Mg^{2+} as the dominant cations; in hot spring waters, the proportion of HCO_3^- decreases, while the relative contributions of SO_4^{2-}, Na^+ and K^+ increase markedly; the charge composition of salt lake brines is highly differentiated, with Cl^- and SO_4^{2-} as the main anions and Na^+ and K^+ as the absolutely dominant cations. Regarding internal variability, the ion composition of general springs is homogeneous with small spatial fluctuations; although hot springs, rivers and freshwater lakes have similar overall concentration levels, some sites show local anomalies in Ca^{2+}, SO_4^{2-} and other components, reflecting the influence of local recharge and water-rock interactions; salt lake brines exhibit the strongest internal heterogeneity, with significant differences in major ion contents, trace element enrichment degrees and dominant anion types among sampling sites, indicating spatial variability in evaporation-concentration intensity and recharge conditions.

 doi:10.20944/preprints202605.1189.v1

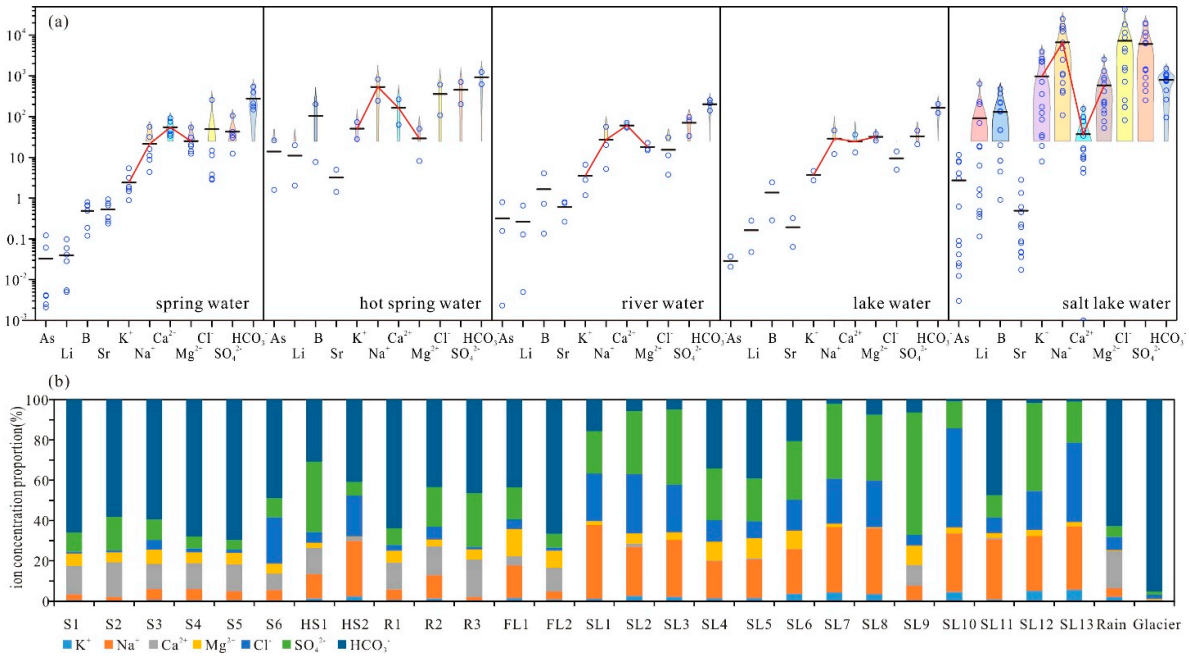

Figure 3. Hydrochemical characteristics of different water bodies in the study area: (a) Ion concentration distribution; (b) Relative ion proportions.

Overall, the water bodies in the study area follow a clear geochemical evolutionary trend: with increasing salinity, ion concentrations increase gradually, anions evolve from HCO_3^- to Cl^- and SO_4^{2-}, cations shift from Ca^{2+}-Mg^{2+} dominance to Na^+-K^+ dominance, accompanied by continuous enrichment of trace elements such as Li, B and Sr. Among these, spatial differentiation is most pronounced in salt lake brines.

4.2. Hydrochemical Types

As shown in Figure 4a, the Piper trilinear diagram, a widely used tool for deciphering major ion compositions and hydrochemical evolutionary characteristics of various water bodies [32,33], clearly illustrates the hydrochemical differentiation of different water types in the study area, including precipitation, glacial meltwater, springs, river water, freshwater lakes, hot springs and saline lakes. Overall, these water types present an orderly spatial evolution from low-salinity end-members to high-salinity end-members. As initial recharge end-members, precipitation and glacial meltwater have extremely low ion contents and are concentrated in the lower-left corner of the diagram, dominated by HCO_3-Ca water, which is mainly controlled by atmospheric deposition and weak rock weathering. Spring and river water samples are distributed in the middle transition zone of the diagram, with hydrochemical types dominated by HCO_3·SO_4-Ca and HCO_3-Ca·Mg; their ion compositions are significantly influenced by water-rock interaction (WRI), with Ca^{2+}, Mg^{2+} and HCO_3^- as dominant species, accompanied by moderate enrichment of Na^+ and Cl^-. Due to the involvement of deep geothermal fluids, hot spring samples exhibit distinctive ion compositions with remarkably high concentrations of Na^+, Ca^{2+} and characteristic components such as Sr, Li, As and B. In contrast, samples from freshwater lakes to saline lakes migrate continuously toward the right and top of the diagram with increasing salinity. Particularly for high-salinity salt lakes such as Laguo Co (SL7), Mami Co (SL10) and Dong Co (SL12), the hydrochemical types gradually transform to Cl-Na and SO_4·Cl-Na types, where evaporation-concentration (EC) replaces rock weathering as the dominant process. Ca^{2+} and Mg^{2+} are relatively depleted due to precipitation of carbonate and sulfate minerals, while Na^+, Cl^- and SO_4^{2-} are continuously enriched. On this basis, the relative ion proportion diagram (Figure 4b) further quantifies the differences in cation and anion compositions among various water bodies. In low-salinity precipitation, glacial meltwater and river water, Ca^{2+} is the dominant cation

 doi:10.20944/preprints202605.1189.v1

and HCO_3^- the dominant anion. With the evolution of water from runoff to lakes, the proportion of Na^+ among cations increases continuously, and Cl^- and SO_4^{2-} gradually replace HCO_3^- as the major anions, consistent with the pattern shown in Figure 3. Hot springs display unique ion allocation characteristics due to high-temperature water-rock reactions.

Collectively, the above patterns reveal a continuous geochemical evolution pathway of water bodies in the study area: starting from recharge by atmospheric precipitation and glacial meltwater, undergoing water-rock interaction during runoff, and finally being controlled by intense evaporation-concentration in closed lake-basin environments.

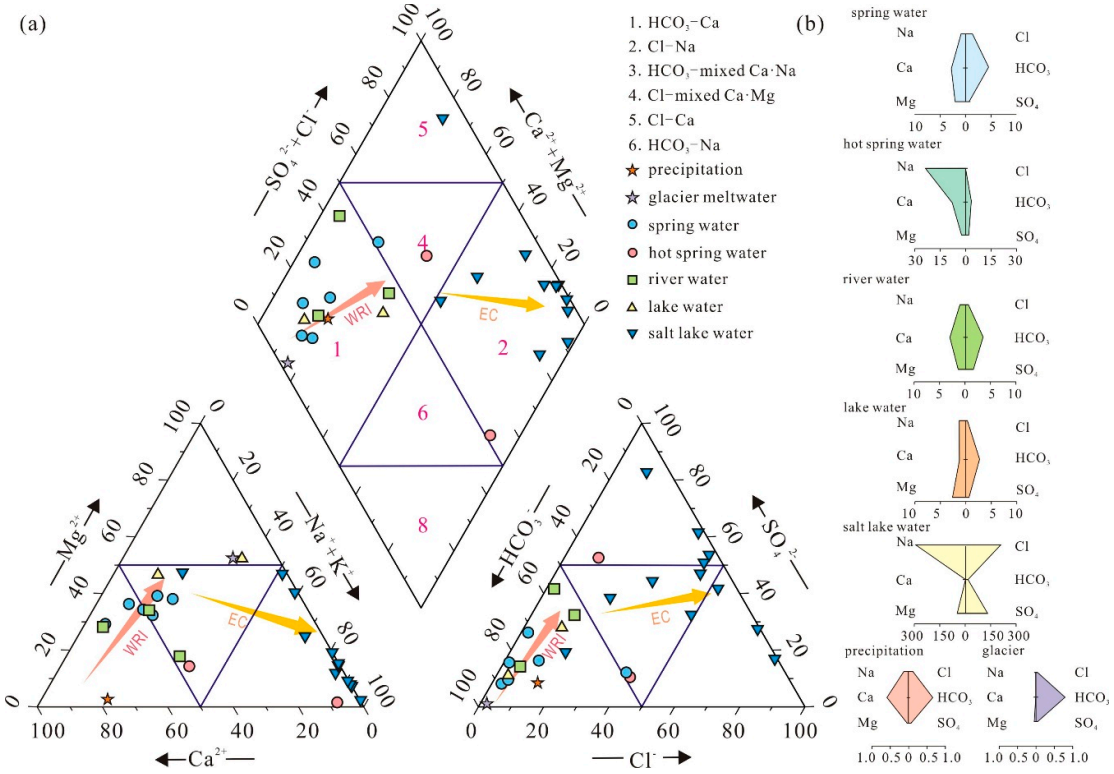

Figure 4. Hydrogeochemical data for different water types in the study area. (a) Piper plot, and (b) Stiff plots for various water types.

5. Discussion

5.1. Hydrochemical Formation Analysis

Lixiviation is the core process of water-rock interaction between groundwater and wall-rock media, and its intensity directly determines the migration and enrichment patterns of hydrochemical components in groundwater [34]. As a classic tool for qualitatively identifying the dominant controlling factors of water ion sources, Gibbs diagrams can intuitively distinguish the contributions of three mechanisms (atmospheric precipitation, rock weathering, and evaporation-concentration) to hydrochemical compositions [35–37]. Water bodies of different types in the study area show distinct zonation characteristics in the Gibbs diagram: precipitation and glacial meltwater samples are concentrated in the lower-left corner of the diagram, with TDS generally below 50 mg/L, and low $Na^+/(Na^+ + Ca^{2+})$ and $Cl^-/(Cl^- + HCO_3^-)$ ratios, falling within the precipitation-dominated zone. River water, spring water and freshwater lake samples are concentrated in the rock weathering-dominated zone of the Gibbs diagram, with TDS mostly ranging from 100 to 1000 mg/L and ion ratios between 0.1 and 0.6, indicating that their hydrochemical characteristics are mainly controlled by weathering and lixiviation of silicate and carbonate rocks in the basin. Hot spring samples have relatively high TDS (>1000 mg/L) and lie near the edge of the rock weathering-dominated zone, suggesting that their

 doi:10.20944/preprints202605.1189.v1

ion compositions are closely related to mineral dissolution during deep high-temperature water-rock interaction. In contrast, saline lake samples migrate significantly toward the evaporation-concentration-dominated zone in the upper-right corner of the diagram. With increasing TDS, both $Na^+/(Na^+{+}Ca^{2+})$ and $Cl^-/(Cl^-{+}HCO_3^-)$ ratios approach 1.0, demonstrating that intense evaporation-concentration is the dominant factor controlling the chemical evolution of salt lake brines. Among them, high-TDS salt lake samples have completely departed from the rock weathering influence zone, with TDS reaching up to the order of 10^5 mg/L, far higher than seawater salinity, revealing the significant modification effect of extreme evaporation on water salinity and ion composition in closed lake-basin environments. In summary, the Gibbs diagram clearly delineates the complete hydrochemical evolutionary sequence of water bodies in the study area, from precipitation recharge, through rock weathering and lixiviation during runoff, to intense evaporation-concentration control in closed lake basins. The distribution characteristics of different water bodies are highly consistent with their recharge sources and the intensity of water-rock interaction (Figure 5).

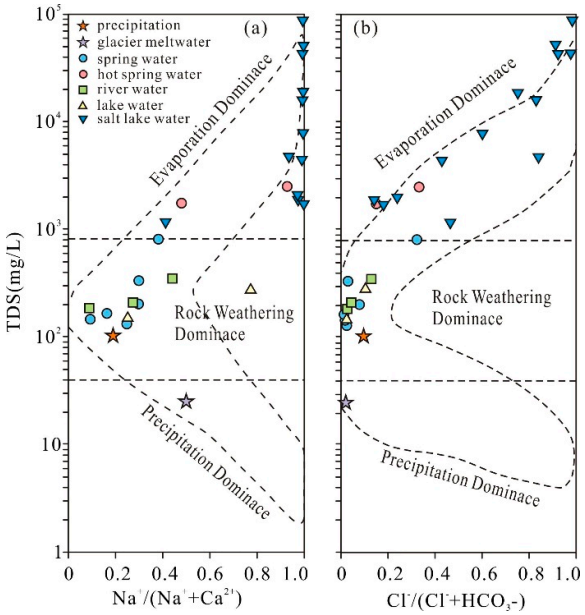

Figure 5. Gibbs diagrams for studied water samples.

In groundwater hydrochemical compositions, the molar ratios of Ca^{2+}/Na^+, Mg^{2+}/Na^+, and HCO_3^-/Na^+ are stable and independent of flow rate, dilution, and evaporation, and are commonly used to qualitatively identify the contributions of carbonate, silicate, and evaporite weathering to solute sources in water bodies [38,39]. As shown in Figure 6, river water, spring water, and most freshwater lake samples are significantly concentrated between the silicate and carbonate end-members, with the majority plotting close to the silicate end-member, indicating that the hydrochemical characteristics of recharge water in the study area are dominated by silicate weathering, while carbonate weathering plays only a secondary role. A small number of hot spring samples are located near the silicate end-member, reflecting the influence of silicate mineral dissolution during deep water-rock interaction. Salt lake brine samples shift distinctly toward the region of low Ca^{2+}/Na^+, low HCO_3^-/Na^+, and low Mg^{2+}/Na^+ in the diagram and form a concentrated zone along the direction of the evaporite dissolution end-member. This suggests that intense evaporation-concentration not only drives the chemical evolution of brines toward the evaporite dissolution trend but also significantly modifies their ionic molar ratios. Specifically, strong evaporation-concentration likely causes the relative depletion of Ca^{2+}, Mg^{2+}, and HCO_3^- due to precipitation of minerals such as calcite and dolomite, resulting in a marked increase in the proportion of Na^+.

 doi:10.20944/preprints202605.1189.v1

In summary, the distributional differences of various water types in the mixing diagram fully present the hydrochemical evolution pathway of the study area: from dominance by silicate and carbonate weathering in the recharge and runoff zones, to modification by intense evaporation-concentration after entering closed lake basins, and finally to the formation of typical brine characteristics. These results further confirm the dual control of rock weathering and evaporation processes on the hydrochemical compositions in the study area.

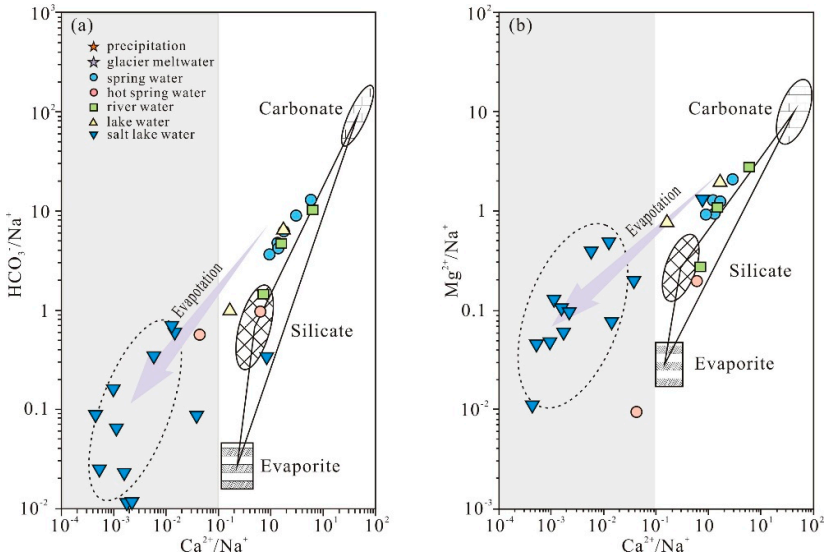

Figure 6. Mixing diagram of the Na-Normalized molar ratios of (a) Ca^{2+}, $HCO_3^-$and (b) Ca^{2+}, Mg^{2+} of each type of water in the study area.

5.2. Typical components Source Analysis

Ionic ratios of hydrochemical components represent a core method for tracing solute sources, migration pathways, and enrichment-evolution mechanisms of water bodies, enabling effective differentiation of the regulatory effects of key hydrogeochemical processes (e.g., rock weathering, evaporation-concentration, and cation exchange) on hydrochemical compositions [40–42]. Based on hydrochemical data of various water types (i.e., atmospheric precipitation, river water, spring water, lake water, and salt lake brine) in the endorheic lake region of the Qiangtang Plateau, systematic insights into the solute sources, genetic mechanisms, and hydrogeochemical evolution patterns of different water bodies in the study area were obtained through correlation analysis between equivalent ratios of major ions and contents of typical trace elements (Figure 7).

The results demonstrated that significant positive correlations were observed between (Na^++K^+) and Cl^-, as well as between (HCO_3^-+SO_4^{2-}) and (Ca^{2+}+Mg^{2+}), for all water samples in the study area, with data points closely aligning along the 1:1 milliequivalent line (Figure 7a,b). This characteristic clearly indicates a high degree of homology between Na^+, K^+ and Cl^-, as well as between Ca^{2+}, Mg^{2+} and HCO_3^-, SO_4^{2-}. The solute components are primarily derived from the weathering and leaching of evaporite and carbonate minerals within the basin, which collectively constitute the dominant material source of solutes in the study area's water bodies.

Meanwhile, except for highly mineralized salt lake brine samples, most sampling sites of other water types (including atmospheric precipitation, river water, spring water, and ordinary lake water) deviated from the 1:1 milliequivalent line to varying extents, generally exhibiting a typical ionic differentiation feature characterized by a weak excess of (Na^++K^+) and a weak depletion of (Ca^{2+}+Mg^{2+}). Combined with the strong negative correlation observed in Figure 7c (coefficient of determination $R^2 = 0.88$), it can be further confirmed that the hydrochemical components in the study area are influenced by cation exchange processes. Specifically, during the migration of water bodies

 doi:10.20944/preprints202605.1189.v1

and their retention in aquifers, highly reactive (Ca^{2+}+Mg^{2+}) in the water undergoes directional exchange with (Na^{+}+K^{+}) adsorbed on the surface of aquifer minerals. This exchange reaction results in a continuous increase in the concentrations of Na^{+} and K^{+}, while the contents of Ca^{2+} and Mg^{2+} in the water decrease relatively.

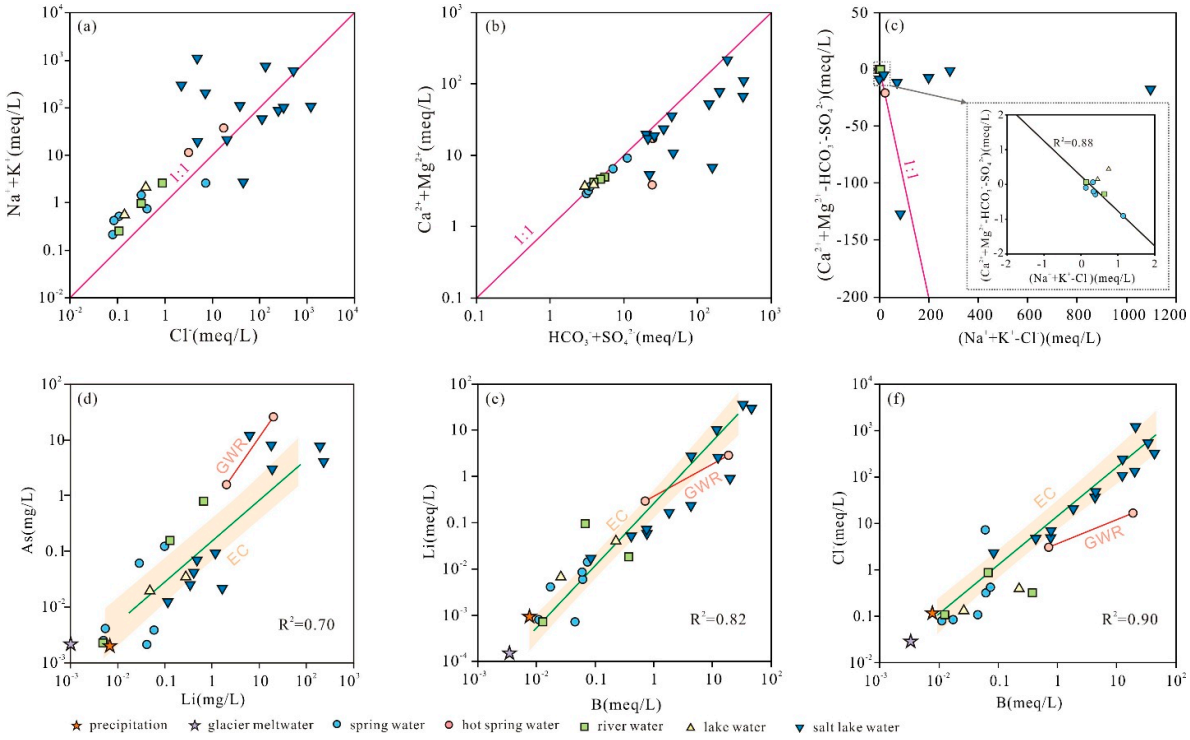

Figure 7. Relationship between major ion concentrations and typical trace elements.

Figures 7(d-f) systematically analyze the coupling relationships between key major ions (e.g., Cl^{-}) and typical trace elements (e.g., As, Li, B). Through three sets of correlation scatter plots (As-Li, Li-B, and Cl^{-}-B), the geochemical differentiation characteristics of different water types during solute evolution are intuitively revealed. The results show that non-hydrothermal water bodies, including precipitation, glacial meltwater, river water, lake water, ordinary spring water, and salt lake brine, are continuously distributed along a high-slope evaporation-concentration (EC) trend line. The coefficients of determination (R^2) of the three diagrams reach 0.70, 0.82, and 0.90, respectively, indicating a good linear coupling relationship. This suggests that under continuous evaporation-concentration, components such as As, Li, B, and Cl exhibit conservative migration characteristics, enriching synchronously with the continuous concentration of water bodies, and the ratios between elements remain relatively stable. These collectively constitute the typical solute enrichment and hydrogeochemical evolution trend of regional shallow water bodies under natural evaporation conditions.

In sharp contrast, hot spring water samples deviate significantly from the aforementioned evaporation-concentration trend line and cluster toward the high-concentration end along a geothermal water mixing (GWR) curve with distinct slope differentiation. This indicates that the hydrochemical components of hot springs are not dominated by shallow evaporation, but rather strongly modified and superimposed by the mixing of deep geothermal fluids. The direct input of deep geothermal fluids not only brings high abundances of characteristic components such as Li, B, As, and Cl^{-}, but also drives intense water-rock interactions in a high-temperature environment, accompanied by the selective dissolution of rock-forming minerals (e.g., silicates and borates) and fluid mixing processes [43,44]. These processes significantly alter the coupling ratios and relative enrichment degrees between elements, ultimately enabling hot spring water to form unique

 doi:10.20944/preprints202605.1189.v1

geochemical component characteristics that are clearly distinguishable from conventional shallow evaporation-dominated water bodies.

The Saturation Index (SI) is a key indicator in hydrogeochemical studies for characterizing the direction and intensity of water-rock interactions, and its value directly reflects whether an aqueous solution is in a state of dissolution, equilibrium, or precipitation with a specific mineral. When SI = 0, the solution reaches dissolution-precipitation equilibrium with the mineral; when SI > 0, the solution is supersaturated, and the mineral tends to precipitate; when SI < 0, the solution is undersaturated, and the mineral will continue to dissolve [45]. Based on the aforementioned geochemical identification criteria, the PHREEQC software was used in this study to calculate the SI values of 12 typical minerals (e.g., anhydrite, aragonite, and calcite) in spring water, river water, hot spring water, freshwater lake water, and salt lake brine in the study area. A boxplot of the saturation index distribution of each mineral in different water types was systematically constructed to intuitively compare the differences and evolutionary trends of water-rock equilibrium states among various water bodies.

The results in Figure 8 clearly indicate that different types of water bodies exert significantly different controlling effects on the mineral dissolution-precipitation equilibrium state. Overall, salt lake brines exhibit the strongest supersaturation characteristics. Silicate minerals such as quartz and talc, as well as carbonate minerals such as calcite and aragonite, all show significantly high SI values. Among them, talc and quartz have the highest degree of supersaturation, which intuitively reflects that under extreme evaporation-concentration conditions, water solutes are highly enriched, and the geochemical conditions for large-scale mineral precipitation have been met. Hot spring water shows obvious differences in characteristics from salt lake brines: its high SI values are mainly concentrated in carbonate minerals (calcite and aragonite) and some silicate minerals, while sulfate minerals such as gypsum and anhydrite are generally in an undersaturated state. This is consistent with the chemical evolution pathway dominated by deep high-temperature water-rock interaction rather than simple evaporation. In contrast, the SI values of most minerals in river water, lake water, and ordinary spring water are close to 0 or lower than 0. In particular, evaporite minerals such as gypsum, anhydrite, and halite are generally undersaturated, indicating that these shallow water bodies are overall in an equilibrium or weak dissolution environment, with weak mineral precipitation.

Notably, calcite, dolomite, and aragonite exhibit a stable weak supersaturation state (SI > 0) in all water bodies, which is a common characteristic of the hydrochemical evolution of various water types in the study area. This indicates that the precipitation of carbonate minerals is a general trend of regional water-rock interaction. Meanwhile, the SI values of calcite and dolomite in hot spring water are significantly higher than those in ordinary spring water, and the degree of undersaturation of gypsum and anhydrite is also higher. This comparison clearly reflects the deep heat source effect brought by the mixing of geothermal water—it not only enhances the precipitation tendency of carbonate minerals but also maintains the dissolution state of sulfate minerals through high-temperature water-rock interaction, forming a clear distinction from salt lake brines dominated by evaporation-concentration.

 doi:10.20944/preprints202605.1189.v1

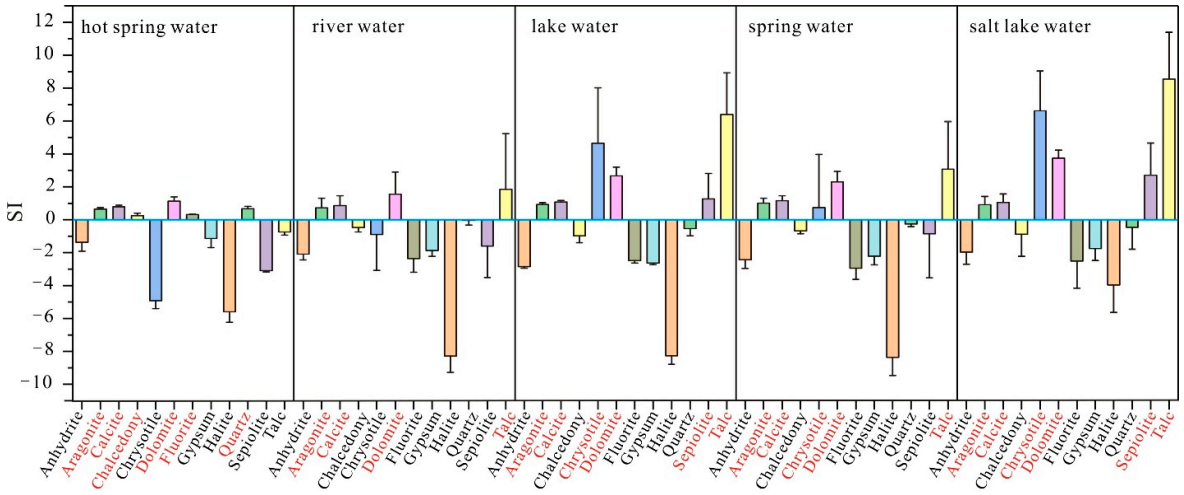

Figure 8. Boxplots of saturation indices (SI) of major minerals across different water types.

5.3. Quantitative Analysis of Controlling Factors

Principal Component Analysis (PCA) is capable of effectively characterizing the overall variation pattern of hydrochemical data via a small number of comprehensive variables, thereby identifying the interrelationships among water ions and their material sources [46,47]. In this study, 28 water samples of different types from the study area were selected as research objects, and a total of 14 hydrochemical indicators—including TDS, As, Li, B, Sr, K^+, Na^+, Ca^{2+}, Mg^{2+}, Cl^-, SO_4^{2-}, HCO_3^-, NO_3^-, and SiO_2—were subjected to PCA to systematically decipher the internal correlations between ions and their dominant geochemical processes. The results indicated that three principal components (F1, F2, F3) with eigenvalues greater than 1 could be extracted from the hydrochemical data of the study area, with a cumulative variance contribution rate of 86.69%, which is sufficient to capture the core information of the original data.

Combined with the Pearson correlation coefficient heatmap and principal component loading plot, TDS was found to be extremely significantly and strongly positively correlated with Na^+, Cl^-, K^+, Li, Mg^{2+}, and SO_4^{2-} ($r > 0.85$, $P < 0.001$), which directly demonstrates that evaporation-concentration is the dominant process governing salinity enrichment in lake basin water bodies. The synergistic enrichment of major ions such as Na^+ and Cl^- is consistent with the typical hydrogeochemical evolution characteristics of arid endorheic lake basins. Li and B also exhibited significant positive correlations with TDS, Na^+, K^+, and Cl^- ($r > 0.62$), indicating that deep water-rock interactions driven by regional tectonic-geothermal activities provide an important material source for the enrichment of characteristic elements. Ca^{2+} showed weak correlations with most salt ions ($r < 0.5$), suggesting that its geochemical behavior is primarily controlled by the dissolution-precipitation equilibrium of carbonate minerals, which is distinctly different from the evaporation-concentration process. SiO_2 was significantly positively correlated with As but not significantly correlated with Li and B, implying that their enrichment is mainly regulated by the weathering and leaching of aluminosilicate minerals, rather than being simply dominated by evaporation-concentration or direct input of deep hot water.

Principal component loading analysis further clarified the contributions of individual hydrochemical processes [48,49]. The first principal component F1 (variance contribution rate: 55.39%) was characterized by high loading indicators, including TDS (loading value: 0.997), Na^+ (0.995), K^+ (0.977), Cl^- (0.951), Mg^{2+} (0.943), Li (0.928), SO_4^{2-} (0.830), NO_3^- (0.806), and B (0.776), which represents evaporation-concentration—the absolute dominant factor in the hydrochemical evolution of the study area. This component reflects the synchronous enrichment of salt ions and representative trace elements resulting from continuous water evaporation under arid climatic conditions. The high loading variables of the second principal component F2 (17.09%) were SiO_2 (0.903), As (0.741), Sr (0.689), and Ca^{2+} (0.514). Among these, the high loadings of SiO_2 and As indicate the leaching and

 doi:10.20944/preprints202605.1189.v1

release of aluminosilicate minerals under high-temperature water-rock interactions, while Sr and Ca^{2+} reflect the dissolution of carbonate minerals, which together constitute the basic material source supply of water ions. The third principal component F3 (contribution rate: 14.21%) was characterized by high positive loadings of Ca^{2+} and Sr, as well as significant negative loadings of As, HCO_3^-, and B, reflecting the coupling process of carbonate dissolution-precipitation and deep fluid mixing. The upward migration of deep hot water triggers CO_2 degassing, which promotes carbonate precipitation and consumes HCO_3^-; B and As are also co-precipitated with minerals [50,51]. Meanwhile, the continuous dissolution of deep carbonate rocks supplements Ca^{2+} and Sr, ultimately forming a hydrochemical assemblage characterized by the enrichment of Ca^{2+} and Sr, and the relative depletion of HCO_3^-, As, and B.

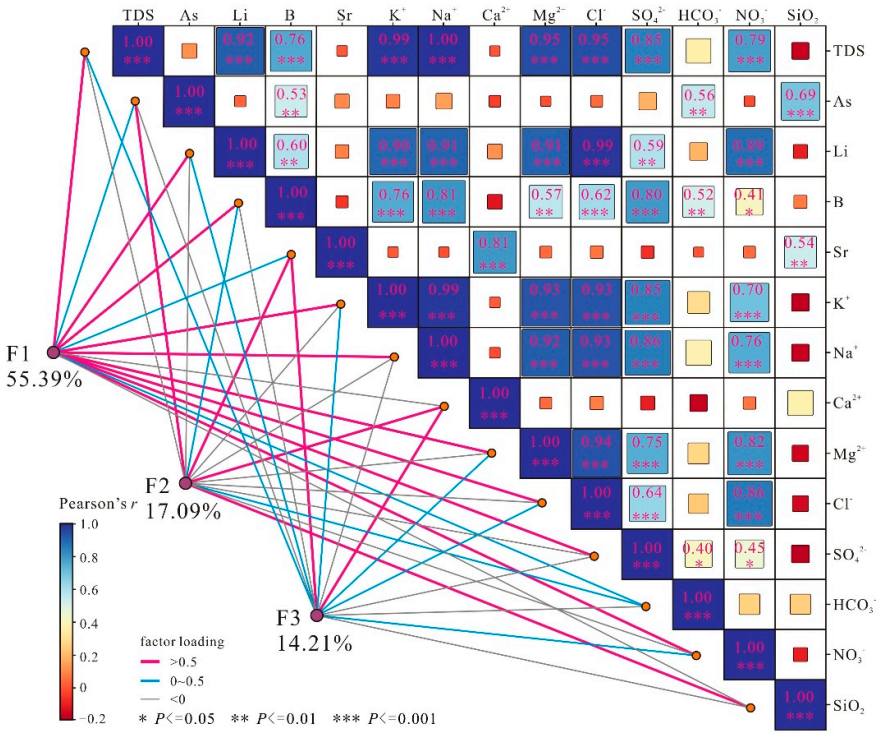

Figure 9. Correlation matrix of hydrochemical parameters and principal component analysis (PCA) loading plot.

Figure 10 shows the contribution rate of each principal component factor to the 14 hydrochemical indicators in water. Among them, the evaporation-concentration process dominated by F1 has a contribution rate exceeding 70% to TDS, K^+, Na^+, Mg^{2+}, Cl^-, Li, and NO_3^-, indicating that evaporation-concentration is the main cause of the enrichment of these ions. The carbonate mineral dissolution and high-temperature aluminosilicate dissolution processes dominated by F2 have a contribution rate exceeding 40% to B, HCO_3^-, As, and SiO_2 components, suggesting that carbonate mineral dissolution and hot water-driven aluminosilicate leaching are the main sources of the above four components. The coupling process of carbonate dissolution-precipitation and deep fluid mixing dominated by F3 has a contribution rate exceeding 40% to Sr, Ca^{2+}, and SiO_2 components, indicating that this coupling process is the main source of the above three components (Figure 10).

 doi:10.20944/preprints202605.1189.v1

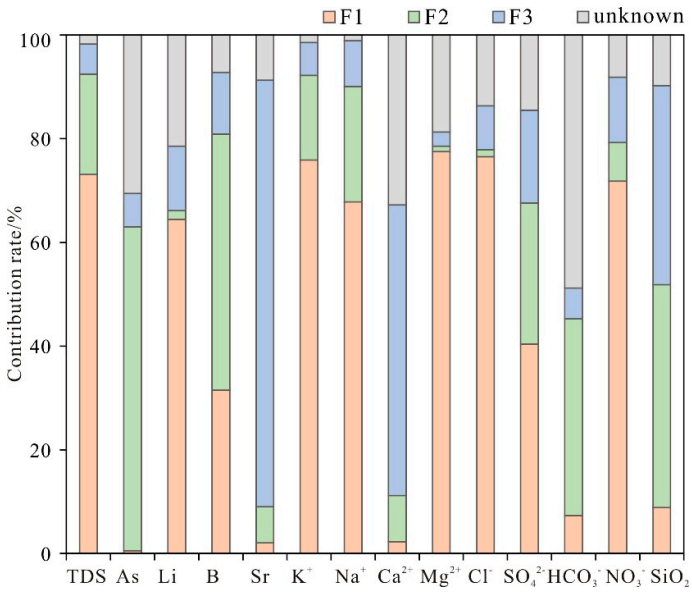

Figure 10. Contribution rates of the principal components (F1, F2, and F3) indices to hydrochemical index.

5.4. Hydrogeochemical Conceptual Model of Solute Enrichment in the Salt Lake Basin on Qinghai-Tibet Plateau

As a typical alpine deep-basin type salt lake distribution area on the Qinghai-Tibet Plateau, the hydrochemical evolution and solute enrichment mechanism of the Qiangtang endorheic lake region are controlled by the comprehensive regulation of multi-source material recharge, water-rock interaction, and evaporation-concentration processes (Figure 11). In the study area, glacial meltwater and atmospheric precipitation serve as the initial recharge sources. After infiltrating and transforming into groundwater, they undergo long-term leaching and water-rock interaction with aquifer surrounding rocks, continuously leaching basic ionic components such as Ca^{2+}, Mg^{2+}, Na^{+}, K^{+}, Sr, and SiO_2 from carbonate and silicate minerals, thus providing initial solute input for the lake basin system.

Deep tectonic zones (e.g., Jenila Suo-Lagala Fault, JL Fault) act as migration channels for geothermal fluids. Magmatic hydrothermal fluids carrying trace elements such as As, Li, and B rise along the fault zones and enter groundwater or river water in the form of hot springs, serving as the core source of rare elements including As, Li, and B. When the high-temperature deep fluids rise to the shallow decompression environment, CO_2 degassing occurs, triggering the precipitation of carbonate minerals such as calcite, and locally forming hydrochemical characteristics of Ca^{2+} and Sr enrichment while HCO_3^{-}, As, and B depletion.

Eventually, groundwater carrying various solutes flows into the salt lake basin. Under the arid climate background of the Qiangtang Plateau, continuous evaporation-concentration occurs, leading to the continuous enrichment of ions such as Na^{+}, K^{+}, Ca^{2+}, Mg^{2+}, Li, and B, and ultimately forming high-solute concentration and high-salinity salt lake brines, completing the entire process of solute migration, transformation, and final enrichment from the source area.

This conceptual model clarifies the hydrogeochemical cycle pathway of "multi-source recharge - water-rock interaction - evaporation-concentration" in the Qiangtang endorheic lake region, providing key theoretical support for revealing the solute enrichment mechanism of salt lake basins in alpine endorheic lake regions and the metallogenic regularity of resources such as lithium and boron.

 doi:10.20944/preprints202605.1189.v1

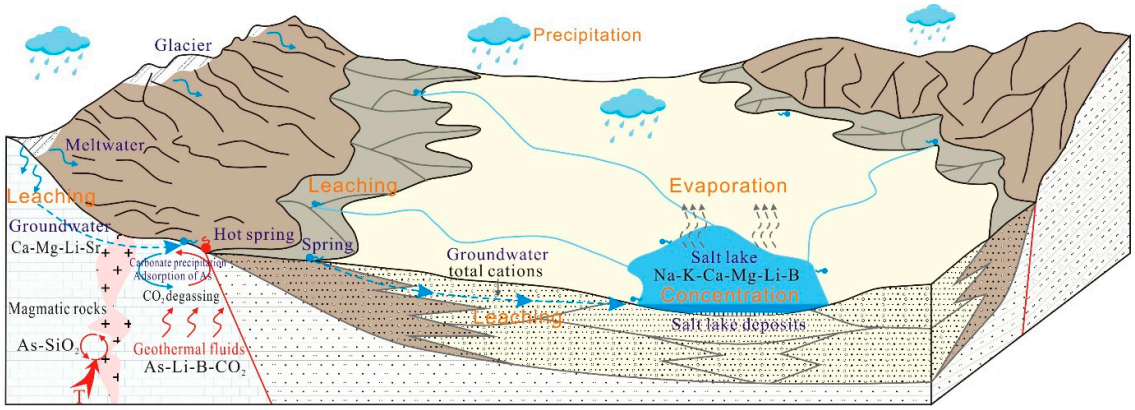

Figure 11. Conceptual model of hydrogeochemical processes controlling solute sources and evolution in the salt lake system.

6. Conclusions

The endorheic lake basin watershed of the Qiangtang Plateau is a typical distribution area of salt lakes enriched in strategic critical metals such as lithium (Li) and boron (B), which is the highest-altitude region of such salt lakes on the Qinghai-Tibet Plateau of China. Conducting research on the solute sources, migration, and enrichment mechanisms of such lake systems is of great scientific significance for revealing the laws of regional hydrogeochemical cycles and guiding the sustainable exploration and development of salt lake resources. Based on the analysis of major ions, trace elements, hydrochemical types, mineral saturation index calculations, and multivariate statistical analysis of samples (including brine, river water, spring water, geothermal water, atmospheric precipitation, and glacial meltwater) in the study area, the following conclusions are drawn:

1. The hydrochemical composition of water bodies in the study area presents a clear gradient evolution law: from atmospheric precipitation and glacial meltwater, through spring water and river water to freshwater lakes, and then to salt lake brine, the total dissolved solids (TDS) increases continuously. Anions are gradually dominated by Cl^- and SO_4^{2-} instead of HCO_3^-, and cations are dominated by Na^+ and K^+ instead of Ca^{2+} and Mg^{2+}, accompanied by significant enrichment of key elements such as Li, B, and Sr.

2. The solute sources and evolution of water bodies are controlled by multiple dominant processes: water bodies in the runoff area are mainly controlled by the weathering and leaching of silicate and carbonate rocks; geothermal water bodies are dominated by deep high-temperature water-rock interaction (WRI) and geothermal fluid input, bringing characteristic trace elements; water bodies in closed lake basins are ultimately modified by extreme evaporation-concentration (EC), which is a key link in solute enrichment and brine formation.

3. As, Li, B, and Cl^- in non-hydrothermal water bodies of the study area show a good linear correlation, enriching synchronously along the evaporation-concentration (EC) trend line with stable element ratios. In contrast, geothermal water samples deviate significantly from the evaporation-concentration trend line and distribute along the geothermal water mixing (GWR) line. Their high contents of Li, B, and As are mainly controlled by deep geothermal fluid input and high-temperature water-rock interaction, forming unique geochemical characteristics distinct from shallow evaporative water bodies.

4. Principal component analysis based on 14 hydrochemical indicators shows that evaporation-concentration (F1, contribution rate of 55.39%) is the absolute dominant factor controlling water salinity and major ion enrichment; the weathering of aluminosilicate and carbonate minerals (F2, 17.09%) provides the basic solute source; the coupling process of deep fluid mixing and carbonate precipitation (F3, 14.21%) plays an important regulatory role in the differentiation of elements such as Ca^{2+}, Sr, B, and As.

 doi:10.20944/preprints202605.1189.v1

Author Contributions: Y.L. and L.Z.: Writing—review and editing; J.C. and T.L.: Writing—original draft; J.F. and Y.G.: Analyzed the chemistry data; Y.L. and X.M.: Project Administration; D.W. and L.L.: Supervision. All authors have read and agreed to the published version of the manuscript. All authors have read and agreed to the published version of the manuscript." Authorship must be limited to those who have contributed substantially to the work reported.

Funding: This research was funded by China Geological Survey, grant number [DD20230424; DD20251237].

Data Availability Statement: Not applicable.

Conflicts of Interest: The authors declare that they have no competing interest.

References

1. Huang, J.; Zhou, X.; Wu, G.; Xu, X.; Zhao, Q.; Liu, Y.; Qie, K. Global climate impacts of land-surface and atmospheric processes over the Tibetan Plateau. *Rev. Geop*hys. **2023**, 61, e2022RG000771.
2. Liu, X.; Sun, H.; Miao, Y.; Dong, B.; Yin, Z.Y. Impacts of uplift of northern Tibetan Plateau and formation of Asian inland deserts on regional climate and environment. *Quat. Sci. Rev*. **2015**, 116, 1–14.
3. Yao, Y.Y.; Zheng, C.M. Groundwater in the Tibetan Plateau: Advances and challenges. Hydrogeol. Eng. Geol. **2025**, 52, 24–33.
4. Wang, X.; Lian, W.H.; Wei, J.F.; Zhang, Y.; Yin, Y.S.; Wang, Q.; Zhang, F.G. Status and problems of water resources on the Qinghai-Tibet Plateau. *Adv. Water Sci.* **2023**, 34, 812–826.
5. Li, Z.; He, M.Y.; Li, B.; Wen, X.; Zhou, J.; Cheng, Y.; Deng, L. Multi-isotopic composition (Li and B isotopes) and hydrochemistry characterization of the Lakko Co Li-rich salt lake in Tibet, China: Origin and hydrological processes. *J. Hydrol*. **2024**, 630, 130714.
6. Zheng, M.P.; Liu, X.F. Hydrochemistry of salt lakes of the Qinghai-Tibet Plateau, China. Aquat. Geochem. **2009**, 15, 293–320.
7. Ding, T.; Zheng, M.; Peng, S.; Lin, Y.; Zhang, X.; Li, M. Lithium extraction from salt lakes with different hydrochemical types in the Tibet Plateau. *Geosci. Front*. **2023**, 14, 101485.
8. Guo, H.M.; Gao, Z.P.; Hu, Y.L.; Xing, S.P.; Li, Y.; Jiang, X.W.; Peng, J.B. Groundwater research in the Tibetan Plateau: Current understanding and key knowledge gaps. *Earth Sci. Front*. **2026**, 33, 328–341.
9. Gaillardet, J.; Dupré, B.; Louvat, P.; Allègre, C.J. Global silicate weathering and CO_2 consumption rates deduced from the chemistry of large rivers. *Chem. Geol*. **1999**, 159, 3–30.
10. Liu, J.; Gao, Z.; Wang, M.; Li, Y.; Shi, M.; Zhang, H.; Ma, Y. Hydrochemical characteristics and possible controls in the groundwater of the Yarlung Zangbo River Valley, China. *Environ. Earth Sci*. **2019**, 78, 76.
11. Li, Y.Z.; Gao, Z.J.; Liu, J.T.; Wang, M.; Han, C. Hydrogeochemical and isotopic characteristics of spring water in the Yarlung Zangbo River Basin, Qinghai-Tibet Plateau, Southwest China. *J. Mt. Sci.* **2021**, 18, 2061–2078.
12. Hu, S.; Zhao, Q.; Wang, G.; Zhang, J.; Feng, J. Hydrochemical Dynamic Characteristics and Evolution of Underground Brine in the Mahai Salt Lake of the Qaidam Basin Qinghai-Tibet Plateau. *Acta Geol. Sin*. **2018**, 92, 1981–1990.
13. He, M.Y.; Cheng, Y.Y.; Chen, J.; Li, Z.Y.; Deng, L.; Ren, T.X.; Rao, H.H. Potassium isotope constraints on brine sources and evolution in Qaidam Basin, Tibetan Plateau. *Ore Geol. Rev*. **2025**, 181, 106632.
14. Tan, H.B.; Chen, J.; Rao, W.B.; Zhang, Y.X. Geothermal constraints on enrichment of boron and lithium in salt lakes: An example from a river-salt lake system on the northern slope of the eastern Kunlun Mountains, China. *J. Asian Earth Sci*. **2012**, 51, 21–29.
15. Ziwen, Z.; Zhifang, Z.; Vanapalli, S.K. A quantitative study of changing groundwater-surface water interactions of a large reservoir due to impoundment based on hydrochemistry and isotope characteristics. *J. Hydrol*. 20**24**, 634, 131092.
16. Sada, D.W.; Thomas, J.M. Relationships between aquatic ecology, landscapes, hydrogeology and hydrochemistry in great basin and Mojave desert spring systems USA. *Ecohydrology* **2025**, 18, e70035.
17. Wang, L.; Xiao, Y.; Yang, H.; Zhang, Y.; Wang, S.; Qi, Z.; Senapathi, V. Formation mechanism of high-altitude glacial mineral water in the Kunlun Mountains of Tibetan Plateau: Insights from isotopes and hydrochemistry. *J. Hydrol. Reg. Stud*. **2024**, 53, 101789.

 doi:10.20944/preprints202605.1189.v1

18. Li, Y.; Bian, J.; Li, J.; Ma, Y.; Anguiano, J.H.H. Hydrochemistry and stable isotope indication of natural mineral water in Changbai Mountain, China. *J. Hydrol. Reg. Stud*. **2022**, 40, 101047.
19. Liu, X.; Xiang, W.; Song, J.; Si, B. Spatial variations in groundwater hydrochemistry, sources, and controls across catchments on Chinese Loess Plateau. *J. Hydrol. Reg. Stud*. **2024**, 53, 101791.
20. Zheng, Y.; Nan, D.; Liu, Z.; Zhao, H.; Zhu, M.; Xing, Y.; Hu, Z. A conceptual model of the hydrochemical evolution and hydrothermal genetics of the geothermal waters of the Ngari Prefecture, Tibet. *Geotherm. Energy* **2025**, 13, 1–29.
21. Song, C.; Huang, B.; Ke, L.; Richards, K.S. Seasonal and abrupt changes in the water level of closed lakes on the Tibetan Plateau and implications for climate impacts. *J. Hydrol*. **2014**, 514, 131–144.
22. Zhou, R.; Zhou, X.; Li, Y.; He, M.; Li, J.; Dong, J.; Luo, Z. Hydrogeochemical and isotopic characteristics of the hot springs in the Litang fault zone, Southeast Qinghai–Tibet plateau. *Water* **2022**, 14, 1496.
23. Shi, Z.; Tan, H.; Xue, F.; Li, Y.; Zhang, X.; Cong, P.; Zhang, Y. Hydrochemical evolution and source mechanisms governing the unusual lithium and boron enrichment in salt lakes of northern Tibet. *Geol. Soc. Am. Bull*. **2024**, 136, 5174–5190.
24. 24 . Xue, F.; Tan, H.B.; Zhang, X.Y.; Li, Y.F.; Cong, P.Y.; Shi, Z.Q. Contrasting sources and enrichment mechanisms in lithium-rich salt lakes: A Li-H-O isotopic and geochemical study from northern Tibetan Plateau. *Geosci. Front*. **2024**, 15, 101768.
25. Li, B.K.; Cheng, H.D.; Ma, H.Z. Boron isotope geochemistry of the Lakkor Co Salt Lake (Tibet) and its geological significance. *Geofluids* **2022**, 3724800.
26. Teng, J.; Yang, D.; Tian, X.; Xu, T.; Chen, Y.; Bai, Z.; Liang, X.; Zhang, X.; Wu, J.; Liu, Y. Geophysical investigation progresses of the Qinghai-Tibetan Plateau in the past 70 years. Sci. Sin. *Terrae* **2019**, 49, 1546–1564.
27. Pan, G.; Li, Z.; Wang, L.; Ding, J.; Chen, Z. Preliminary division of tectonic units of the Qinghai-Tibet Plateau and its adjacent regions. *Geol. Bull. China* **2002**, 21, 702–707.
28. Sichuan Geological Survey. Regional Geological Survey Report of the People's Republic of China (1:250,000 Wuma Sheet); Sichuan Geological Survey: Chengdu, China, **2005.**
29. Ding, L.; Kapp, P.; Cai, F.; Dong, H.; Fu, B.; Gupta, A.; Huang, W.; Liu, S.; Ma, Y.; Meade, B.; et al. Timing and mechanisms of Tibetan Plateau uplift. Nat. Rev. *Earth Environ*. **2022**, 3, 652–667.
30. Zhou, J.; Li, B.; He, M.; Jiao, J.; Tang, Z.; Li, Z. Hydrochemical characteristics and sources of lithium in carbonate-type salt lake in Tibet. *Sustainability* **2023**, 15, 16235.
31. Zhou, J.; He, M.; Li, B.; Jiao, J.; Tang, Z.; Li, Z.; Rao, H. Lithium isotopic composition of the carbonate type salt lake in Tibet and its implication for origin and hydrological processes. *Sci. Rep*. **2025**, 15, 11862.
32. Ma, W.J.; Wang, W.K.; Hou, X.X. Spatial evolution of hydrogeochemistry driven by river water-groundwater transformations in the Manas River Basin. Bull. *Geol. Sci. Technol*. **2025**, 44, 378–388.
33. Liu, Q.; Zhang, Z.; Zhang, B.; Mu, W.; Zhang, H.; Li, Y.; Xu, N. Hydrochemical analysis and identification of open-pit mine water sources: A case study from the Dagushan iron mine in Northeast China. *Sci. Rep*. **2021**, 11, 23152.
34. Li, Z.J.; Yang, Q.C.; Yang, Y.S.; Ma, H.; Wang, H.; Luo, J.N.; Bian, J.M.; De-Miguel, J. Isotopic and geochemical interpretation of groundwater under the influences of anthropogenic activities. *J. Hydrol*. **2019**, 576, 685–697.
35. Gibbs, R.J. Mechanisms controlling world water chemistry. Science **1970**, 170, 1088–1090.
36. Andres, M.; Paul, S. Groundwater chemistry and the Gibbs Diagram. *Appl. Geochem*. **2018**, 97, 209–212.
37. Hou, Q.; Pan, Y.; Zeng, M.; Wang, S.; Shi, H.; Huang, C.; Peng, H. Assessment of groundwater hydrochemistry, water quality, and health risk in Hainan Island, *China. Sci. Rep*. **2023**, 13, 12104.
38. Wu, Y.; Gibson, C.E. Mechanisms controlling the water chemistry of small lakes in northern Ireland. *Water Res*. **1996**, 30, 178–182.
39. Wang, L.; Xiao, Y.; Yang, H.; Zhang, Y.; Wang, S.; Qi, Z.; Senapathi, V. Formation mechanism of high-altitude glacial mineral water in the Kunlun Mountains of Tibetan Plateau: Insights from isotopes and hydrochemistry. *J. Hydrol. Reg. Stud*. **2024**, 53, 101789.
40. Ma, R.; Wang, Y.X.; Sun, Z.Y.; Zheng, C.M.; Ma, T.; Prommer, H. Geochemical evolution of groundwater in carbonate aquifers in Taiyuan, northern China. Appl. *Geochem*. **2011**, 26, 884–897.

 doi:10.20944/preprints202605.1189.v1

41. Liu, Y.; Zhou, L.; Ma, X.; Li, W.; Li, J. Comprehensive study of groundwater hydrochemistry, driving forces, and health risks in representative rural agglomerations, Northern China. *ACS Omega* **2025**, 10, 18391–18403.
42. Pu, J.B.; Yuan, D.X.; Xiao, Q.; Zhao, H.P. Hydrogeochemical characteristics in karst subterranean streams: A case history from Chongqing, China. *Carbonates Evaporites* **2015**, 30, 307–319.
43. Lü, Y.; Zheng, M.; Zhao, P.; Xu, R. Geochemical processes and origin of boron isotopes in geothermal water in the Yunnan-Tibet geothermal zone. Sci. *China Earth Sci*. **2014**, 57, 2934–2944.
44. Kasemann, S.A.; Meixner, A.; Erzinger, J.; Viramonte, J.G.; Alonso, R.N.; Franz, G. Boron isotope composition of geothermal fluids and borate minerals from salar deposits (central Andes/NW Argentina). *J. S. Am. Earth Sci*. **2004**, 16, 685–697.
45. Pu, J.B.; Yuan, D.X.; Jiang, Y.J.; Gou, P.F.; Yin, J.J. Hydrogeochemistry and environmental meaning of Chongqing subterranean karst streams in China. *Adv. Water Sci*. **2010**, 21, 628–636.
46. Shafiullah, G.; Al-Ruwaih, F.M. Spatial-multivariate statistical analyses to assess water quality for irrigation of the central part of Kuwait. *Bull. Eng. Geol. Environ*. **2020**, 79, 27–37.
47. Tian, H.; Du, J.Z.; Sun, Q.F.; Zhang, Y. Evaluation of shallow groundwater for drinking purpose based on water quality index and synthetic pollution index in Changchun New District, China. Environ. *Forensics* **2021**, 22, 189–204.
48. Abou Zakhem, B.; Al-Charideh, A.; Kattaa, B. Using principal component analysis in the investigation of groundwater hydrochemistry of Upper Jezireh Basin, Syria. *Hydrol. Sci. J*. **2017**, 62, 2266–2279.
49. Ravikumar, P.; Somashekar, R.K. Principal component analysis and hydrochemical facies characterization to evaluate groundwater quality in Varahi river basin, Karnataka state, India. Appl. *Water Sci*. **2017**, 7, 745–755.
50. Liu, M.L.; Zheng, A.T.; Shang, J.B.; Guo, Q.H. Progress in Study of Boron Geochemistry in High Temperature Geothermal Fluids. *J. Earth Sci*. **2023**, 48, 878–893.
51. McGrory, E.; Holian, E.; Alvarez-Iglesias, A.; Bargary, N.; McGillicuddy, E.J.; Henry, T.; Morrison, L. Arsenic in groundwater in south west Ireland: Occurrence, controls, and hydrochemistry. *Front. Environ. Sci.* **2018**, 6, 154.